C201 Viscous Flow and Turbulence

Lecture 3

Part 1: Linear eddy viscosity models

Luca di Mare

St John's College

1 The RANS equations and the closure problem

In previous chapters we have examined in detail the implications of the RANS for parallel shear flows such as jets, wakes and boundary layers.

We have obtained scaling laws for jets and wakes and a closed-form expression for the velocity profile in a part of a boundary layer using order-of magnitude estimates for the Reynolds stress or dimensional arguments.

We now turn our attention to techniques used to model more general flows. The main obstacle to overcome in applying the Reynolds equation to general flows is the closure problem: we don't generally know the distribution of the Reynolds stress tensor.

The closure problem is overcome by employing empirical models relating the mean properties of the flow – made available by the solution of the RANS equation – to the Reynolds stress distribution. Such models are collectively known as turbulence models.

The empiricism in turbulence models is made necessary by the fact the the Reynolds stress distribution is determined in part by small scales of motion, but these are inaccessible in RANS calculations.

Once closed with a suitable turbulence model, the RANS equations become – in principle at least - a well posed set of non-linear partial differential equations that can be approximated with standard techniques of numerical analysis and can be used to compute approximations of the flow field past bodies of arbitrary shape. Despite their theoretical limitations, turbulence models perform reasonably well for many flows of practical interest and for this reason are an invaluable engineering tool.

1.1 Origin of the Reynolds stress

We have mentioned previously that the Reynolds stress arises because of the correlation between velocity components induced at a give location by the presence of flow structures – i.e. eddies.

In this lecture we are particularly interested in the Reynolds shear stress, because it is responsible for the transfer of momentum in parallel shear flows.

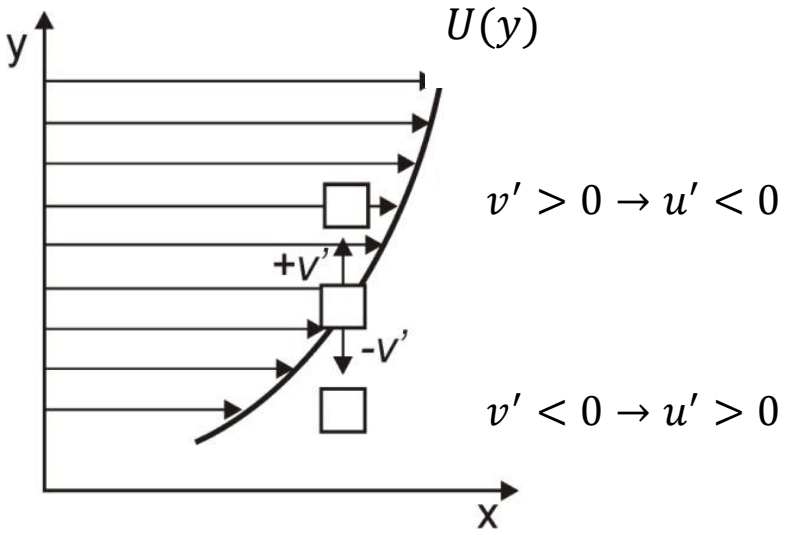

Figure 1: formation of the Reynolds shear stress across a mean velocity gradient

Without loss of generality we can consider a statistically two-dimensional flow with no mean velocity along the y-axis. If there is a velocity gradient (e.g. $\frac{dU}{dy} > 0$ like in Figure 1), then passing eddies induce a negative correlation between the velocity components u' and v'. To see how this happens, let us consider an eddy that causes a positive vertical velocity perturbation, $v' > 0$. On average, the fluid leaving a give position y will be transferred to a location where the velocity is higher – by virtue of the mean velocity gradient – and therefore it will appear as a negative streamwise velocity perturbation u'.

Similar reasoning leads us to the conclusion that if $v' < 0$ the $u' > 0$. We see then that there must be a Reynolds stress $\overline{u'v'} < 0$ associated with the velocity gradient $\frac{dU}{dy} > 0$.

Our argument is valid in most ordinary turbulent flows and we will see later that it leads to reasonable and useful conclusions about the Reynolds stress distribution.

We should not forget, however, that our argument is somewhat limited in validity because it assumes that parcels of fluid are to positions where the local mean velocity is not too different from the velocity at position y. We are also neglecting the shape of the instantaneous velocity profile: it is perfectly possible that, while $\frac{dU}{dy} > 0$, from time to time and in certain locations we could have $\frac{du}{dy} < 0$.

2 Boussinesq's hypothesis

Before we venture further into the topic of turbulence modelling, we must make a short detour to look back at molecular viscosity in ideal gas. The kinetic theory of dilute gases describes viscosity as arising from the redistribution of linear momentum caused by collision between pairs of molecules.

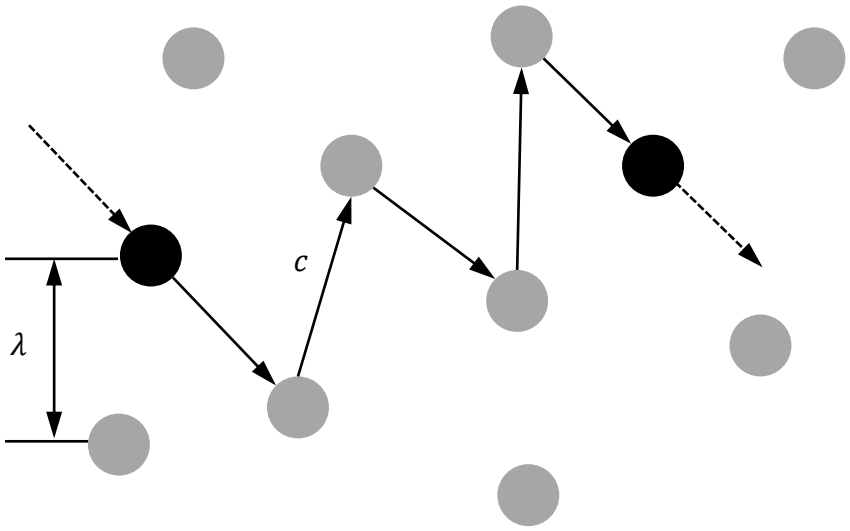

Figure 2

The kinematic viscosity of an ideal gas is proportional to the average distance between collisions – the mean free path – and the speed between consecutive collisions.

The resulting expression for the kinematic viscosity of an ideal gas is

$$\nu \propto \lambda\, c$$

Let us know replace molecules with turbulent eddies. If the turbulent eddies follow a random walk of the type postulated by the kinetic theory, then a turbulent flow field idealised as an ideal gas of eddies should exhibit a kinematic “eddy” viscosity proportional to the mean velocity between consecutive collisions and the average distance between collisions.

The mean velocity must scale with the TKE

$$u' \propto \sqrt{k'}$$

The distance between “collisions” corresponds to the distance travelled by a turbulent eddy before it mixes with its surroundings. We shall call this distance the mixing length

$$\ell_{mix}$$

The eddy viscosity must scale – by analogy with the kinetic theory of gases – as

$$\nu_T \propto \ell_{Mix} u'$$

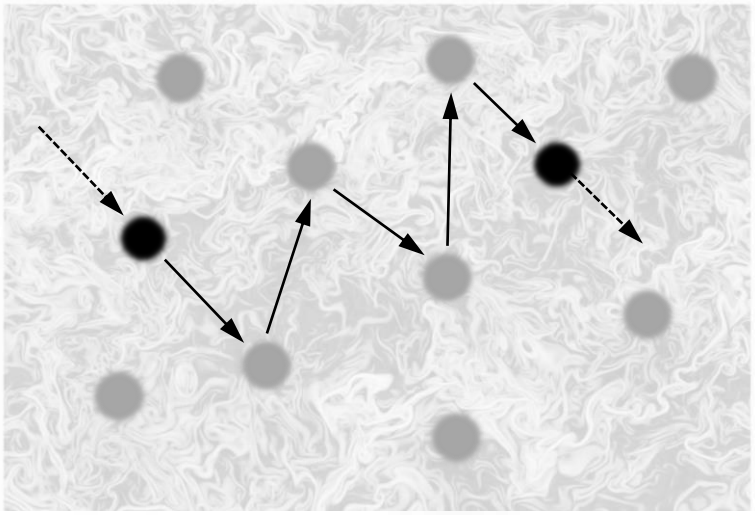

Figure 3

It is tempting now to write that the Renolds stress can be related to the mean shear by an expression similar to the constitutive relation of a Newtonian fluid:

$$\overline{u_i' u_j'} \approx -2\nu_T \left(\frac{\partial U_i}{\partial x_j} + \frac{\partial U_j}{\partial x_i} \right) + \frac{2}{3} \delta_{ij}\, k$$

This equation is the formal statement of Boussinesq's hypothesis: the Reynolds stress proportional to mean shear through a coefficient called eddy viscosity. Boussinesq's hypothesis is a fairly crude empirical approximation. It can be proven to be in error even for relatively simple flows, but it is sufficiently accurate to form the bases of many phenomenological turbulence models.

2.1 Linear Eddy viscosity models

The models applying directly Boussinesq's hypothesis to obtain a constitutive relation for the Reynolds stress are known collectively as linear eddy viscosity model. The adjective "linear" refers to the linear nature of the relation between stress and strain, mediated by the eddy viscosity.

$$\overline{u_i' u_j'} \approx -2\nu_T \left(\frac{\partial U_i}{\partial x_j} + \frac{\partial U_j}{\partial x_i} \right) + \frac{2}{3} \delta_{ij}\, k$$

The differences between the models are determined by the way each of them tries to infer the value of ν_T from the mean flow. As we have seen earlier, ν_T necessitates an estimate of the mixing length and an estimate of the turbulence intensity. This information is obtained in a number of different ways:

- Algebraic models: ν_T inferred from algebraic relations involving velocity gradient and geometric quantities (e.g. distance from the wall)
- 1 equations models: transport equation for ν_T(or equivalent quantity)

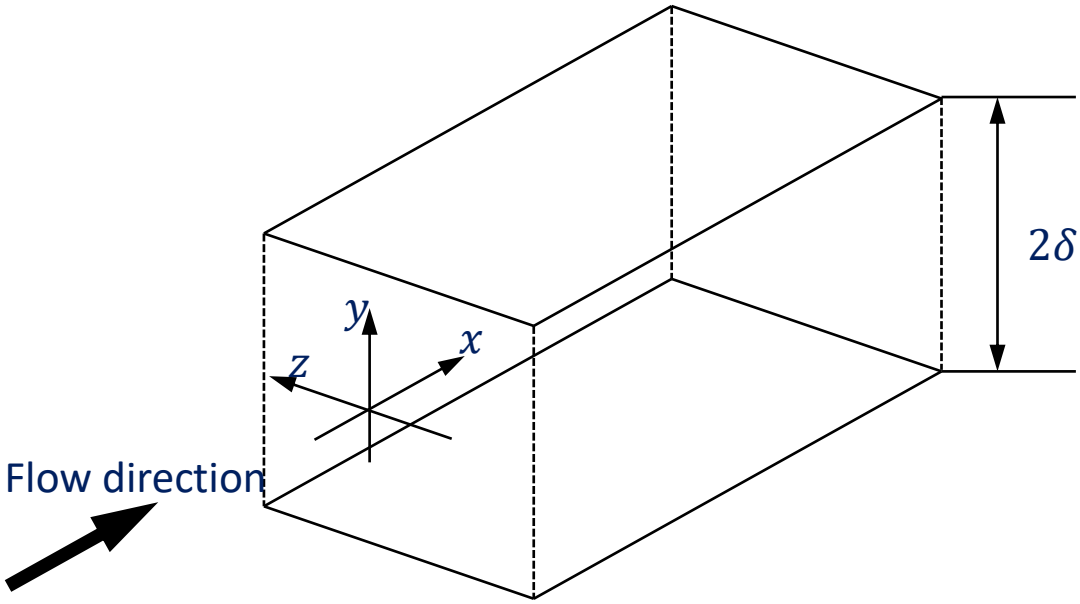

Figure 4: Coordinate system for the turbulent channel flow

- 2 equation models: transport equations for k (TKE) and quantity related to length scale (dissipation rate, specific dissipation rate etc.)
-

3 The turbulent channel flow

We will need in our exposition of turbulent models a flow that is at the same time sufficiently simple to allow us some analytical estimates but also representative of flows of practical interest. We will use this flow to show the predictive ability – or lack thereof – of the turbulence models we will present and also to illustrate in detail the variation of quantities of interest in the model.

Such a flow is the turbulent channel flow. The turbulent channel flow is an idealised turbulent flow taking place between parallel plates of infinite extent. The plates are placed at a distance 2δ. A convenient frame of reference for the study of turbulent channel flow is shown in Figure 4. We take the x axis aligned with the mean flow direction, the y axis orthogonal to the wall and the z axis in the direction orthogonal to both x and y. The flow is statistically uniform in the directions x (streamwise) and z (spanwise). The flow is sustained by a pressure gradient that acts in the negative x direction. The force applied by the pressure gradient to any section of the flow is balanced by the shear stress at the wall. A simple momentum balance shows that

$$-\frac{\delta}{\rho}\frac{dP}{dx} = \frac{\tau_w}{\rho} = u_\tau^2$$

We defined u_τ when we introduced turbulent boundary layers as a velocity scale representing the wall shear stress τ_w.

The flow is entirely described by the variation of the streamwise velocity U along y. A flow very similar to turbulent channel flow is realised between the plates of heat

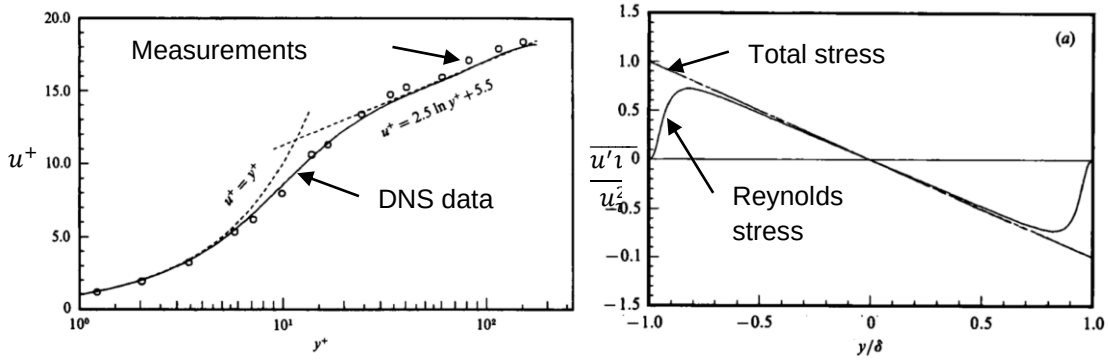

Figure 5: Mean velocity and Reynolds stress profiles in turbulent channel flow at $Re_\tau = 180$, from Kim, J., Moin, P., & Moser, R. (1987). Turbulence statistics in fully developed channel flow at low Reynolds number. *Journal of Fluid Mechanics, 177*, 133-166.

exchangers. The velocity profiles and turbulence statistics in pipes as well as boundary layers with mild pressure gradients resemble very closely those in turbulent channel flows.

3.1 The RANS equation for turbulent channel flow

Only one momentum equation is sufficient to describe the turbulent channel flow:

$$0 = \nu \frac{d^2U}{dy^2} - \frac{d\,\overline{u'v'}}{dy} - \frac{1}{\rho}\frac{\mathrm{dP}}{\mathrm{dx}}$$

If we normalize lengths by the channel half-width δ and velocities by the friction velocity u_τ we find in non-dimensional form:

$$\frac{1}{Re_\tau}\frac{d^2u^+}{d\eta^2} - \frac{d}{d\eta}\frac{\overline{u'v'}}{u_\tau^2} + 1 = 0$$

where

$$\eta = y/\delta$$

$$u^+ = U/u_\tau$$

and

$$Re_\tau = \frac{u_\tau \delta}{\nu}$$

3.2 Mean velocity and stress profiles for turbulent channel flows

Because of its geometric simplicity and its technical interest, the turbulent channel flow has been intensely studied and it is one of the first flows for which a direct numerical simulation (DNS) was conducted. Results from one of the first DNS of turbulent channel flow are reported in Figure 5. It can be seen that the mean velocity profile obeys the universal law of the wall. The total stress in a channel flow is a linear function of the y coordinate. This is a consequence of the fact that the divergence of the stress balances the pressure gradient, which is constant.

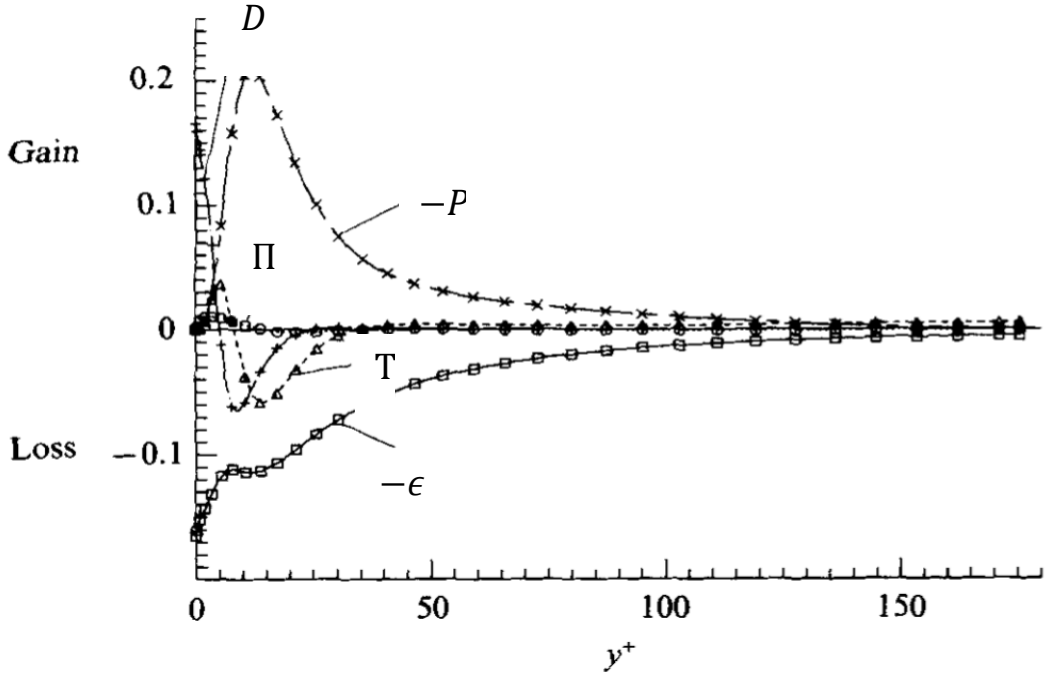

Figure 6: TKE budget in turbulent channel flow at $Re_\tau = 180$, from Mansour, N., Kim, J., & Moin, P. (1988). Reynolds-stress and dissipation-rate budgets in a turbulent channel flow. *Journal of Fluid Mechanics, 194*, 15-44.

As a consequence, the Reynolds stress is linear away from the wall – where the viscous stress cannot contribute to momentum transfer - but decays to 0 at the walls, where it is the viscous stress that balances the pressure gradient.

3.3 TKE budget in turbulent channel flows

The availability of DNS data meant that the turbulent channel flow is also one of the earliest flows for which detailed distributions of the terms in the TKE budget are known. We recall the TKE budget from lecture 1 and we rearrange it as

$$0 = \underbrace{-\frac{1}{\rho}\overline{u_i'\frac{\partial p'}{\partial x_i}}}_{\Pi} + \underbrace{\nu\frac{\partial^2 k}{\partial x_j \partial x_j}}_{D} - \underbrace{\nu\overline{\frac{\partial u_i'}{\partial x_j}\frac{\partial u_i'}{\partial x_j}}}_{\epsilon} - \underbrace{\frac{\partial}{\partial x_j}\overline{u_j' u_i' u_i'}}_{T} - \underbrace{\overline{u_i u_j'}\frac{\partial U_i}{\partial x_j}}_{P}$$

We recall that Π represents the correlation between velocity fluctuations and pressure gradients, D is the viscous diffusion of TKE, T is the turbulent diffusion of TKE, P is the production of TKE at the expense of the mean flow and ϵ is the dissipation rate. In a turbulent channel flow P only has one contribution

$$P = \overline{u'v'}\frac{dU}{dy}$$

The variation of the budget terms computed by Mansour et al at $Re_\tau = 180$ is shown in Figure 6. We can see that away from the wall ($y^+ > 50$) the turbulent channel flow is an equilibrium flow with TKE production matching the dissipation rate. Closer to

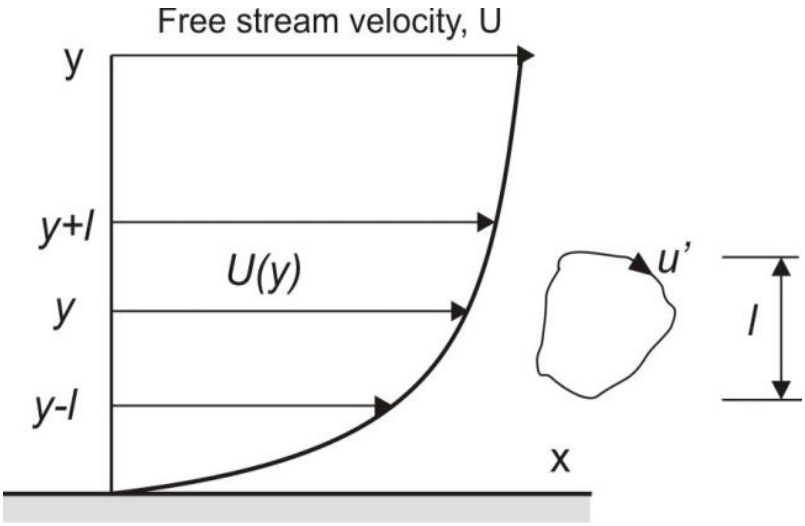

Figure 7

the wall the production has a peak around $y^+ \sim 20$ and then decays rapidly approaching the wall. In the region between the wall and the peak production, turbulence is destroyed by the dissipation – which has a finite limit at the wall – and is sustained by diffusion, both turbulent and viscous.

4 Algebraic (Zero-Equation) models: Prandtl's mixing length

The simplest turbulence mode is Prandtl's mixing length model. The model is a straightforward application of the kinetic argument proposed earlier but it contain a further observation about how to obtain an estimate for u'.

The observation is that if u' must scale like the velocity difference between points separated by a distance ℓ_{Mix}

$$u' \sim U(y + \ell_{Mix}) - U(y)$$

If ℓ_{Mix} is small compared to the geometric scale of the flow then a Taylor expansion suggets

$$U(y + \ell_{Mix}) \approx U(y) + \ell_{Mix} \frac{\partial U}{\partial y}$$

Which leads to the following estimate for the turbulent velocity scale:

$$u' \sim \ell_{Mix} \left| \frac{\partial U}{\partial y} \right|$$

Using Boussinesq's hypothesis we find for the Reynolds stress:

$$\overline{u'v'} \sim -\ell_{Mix}^2 \left| \frac{\partial U}{\partial y} \right| \frac{\partial U}{\partial y}$$

Because ℓ_{Mix} is the only variable available to modulate the eddy viscosity, Prandtl's mixing length model and its derivatives seek to build geometric model for ℓ_{Mix}

For general three-dimensional flows the model is generalised by the following constitutive law:

$$\tau_{ij} = \left(\mu + \rho \ell_{Mix}^2 \max_{i \neq j} \left|\frac{\partial U_i}{\partial x_j}\right|\right)\left(\frac{\partial U_i}{\partial x_j} + \frac{\partial U_j}{\partial x_i}\right)$$

The model performs well in parallel shear flows and boundary layers with moderate pressure gradient and no flow separation.

In boundary layers, $\ell_{Mix} \approx 0.41\, y$ here y is the distance to the wall.

For free shear flows:

- $\ell_{Mix} = 0.07d$ for a plane mixing layer,
- $\ell_{Mix} = 0.09d$ for a plane jet and
- $\ell_{Mix} = 0.075d$ for a round jet.

In practice ℓ_{Mix} is limited by physical considerations: the integral scale must be limited and the mixing length can't be larger than the integral scale. Information about the maximum value of the mixing length is usually available empirically and is typically related to the dimensions of the flow geometry. The largest mixing length also depends on the history of the flow, the pressure gradient etc.

$$\ell_{Mix} = \min(\kappa y, \ell_{Max})$$

The mixing length expression above is not suitable for calculation where the viscous layer is discretized. Within the viscous layer the Reynolds stress must disappear despite the finite velocity gradient. This behaviour can be accomplished by introducing a corrective factor which depends on the distance from the wall. An example of such factor is the van Driest "damping":

$$\ell_{Mix} = \min(\kappa y, \ell_{Max})(1 - e^{-y^+/26})$$

The model above is usually known as Cebeci's algebraic model.

4.1 Implications of the mixing length model in turbulent channel flows

In a turbulent channel flow let y' be the distance from the lower wall:

$$y' = \delta + y$$

and η'its associate non-dimensional coordinate

$$\eta' = y'/\delta$$

The mixing length model with $\ell_{Mix} = \kappa y'$ becomes

$$\nu_T = \ell_{Mix}^2 \left|\frac{\partial U}{\partial y}\right| = \kappa^2 y'^2 \left|\frac{dU}{dy}\right|$$

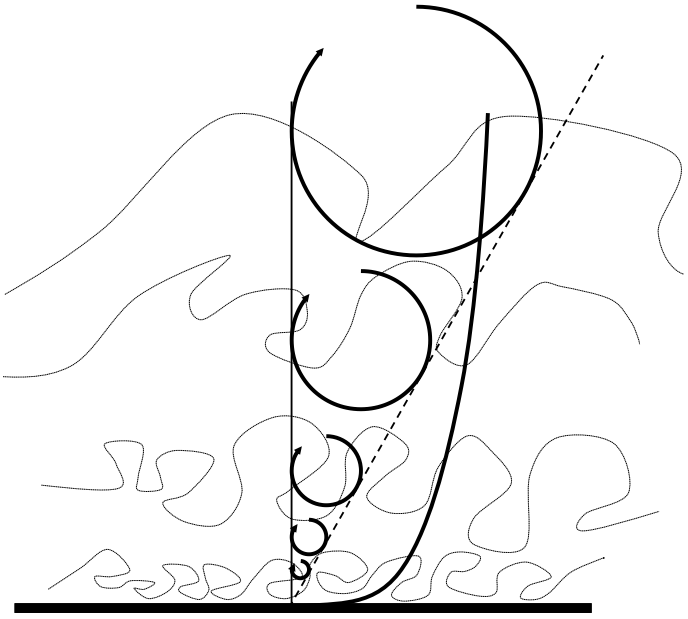

Figure 8: a linear eddy viscosity implies eddies of size directly related to the distance from the wall

and the corresponding expression for the Reynolds shear stress is

$$\tau = -\kappa^2 y'^2 \left(\frac{dU}{dy} \right)^2$$

Recalling the RANS equation, we can substitute y' for y and η' for η in the derivatives to find

$$\frac{1}{Re_\tau} \frac{d^2 u^+}{d\eta'^2} - \frac{d}{d\eta'} \frac{\overline{u'v'}}{u_\tau^2} + 1 = 0$$

Taking the limit of high Reynolds number, i.e. $Re_\tau \to \infty$ yields

$$-\frac{d}{d\eta'} \frac{\overline{u'v'}}{u_\tau^2} = 1$$

At the center of the channel $\eta' = 1$ and $\tau = \overline{u'v'} \to 0$ therefore integration gives

$$\frac{\overline{u'v'}}{u_\tau^2} = 1 - \eta'$$

Substituting the mixing length estimate for the Reynolds stress gives

$$\kappa^2 \eta'^2 \left(\frac{du^+}{d\eta} \right)^2 = 1 - \eta'$$

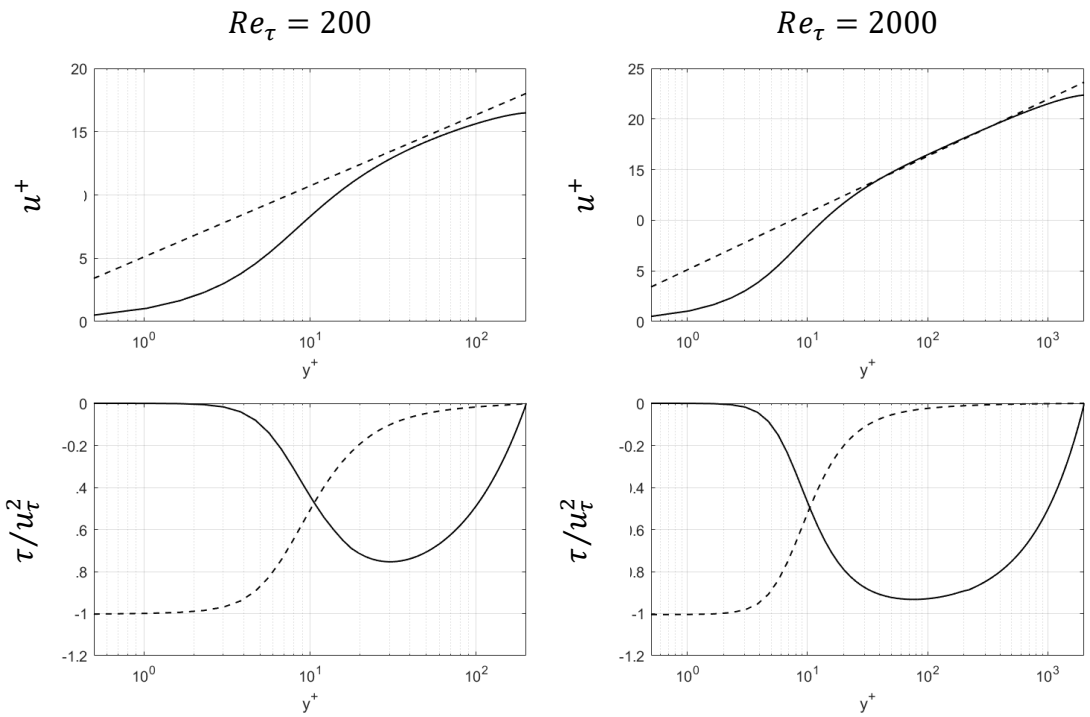

Figure 9: mean velocity profile and stress distributions from Cebeci's model for turbulent channel flow at Re_τ 200 and 2000.

Close to the wall $\eta \to 0$ (but not so close that viscous stress becomes large again!)

$$\frac{du^+}{d\eta'} = \frac{1}{\kappa\eta'}$$

Integrating gives us the logarithmic law of the wall we found from dimensional arguments in the previous lecture:

$$u^+ = \frac{1}{\kappa}\log\eta' + C = \frac{1}{\kappa}\log y^+ + \beta$$

This result is very important: it shows that the logarithmic law of the wall is a direct consequence of the variation of the mixing length with the distance from the wall. The linear variation

$$\ell_{Mix} = \kappa y$$

is in fact a statement about the size of the eddies producing the Reynolds stress: they must grow in size as we move away from the wall or, conversely, their size is limited by their distance from the wall (see Figure 8).

4.2 Turbulent channel flow with Cebeci's model

Figure 9 shows velocity and stress distributions for turbulent channel flow obtained with Cebeci's model (more in the Activities section). The model has been applied at $Re_\tau = 200$ and at $Re_\tau = 2000$. The results at lower Reynolds number contain significant departures from the log-law profile. This is not unexpected: the derivation in the previous section indicated that the appearance of the log-law requires us to be

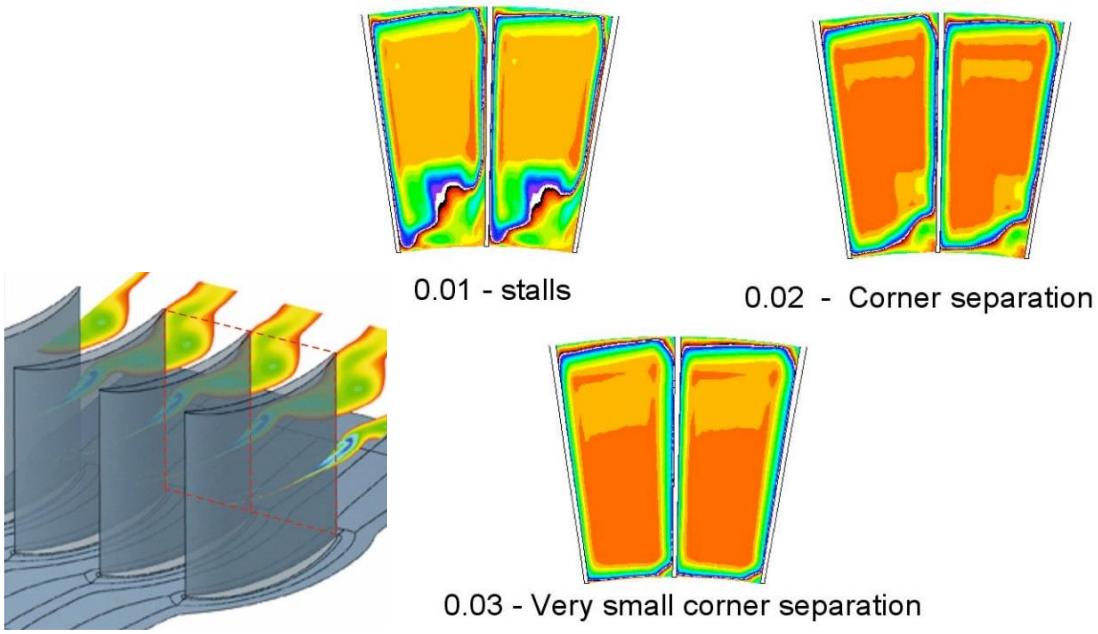

Figure 10: effect of the selection of maximum mixing length on the flow through a compressor passage, after J. D. Denton, GT2010-22540.

at the same time outside the viscous layer but at a small distance from the wall. At low Reynolds number these two conditions become difficult to reconcile. We also notice that the model correctly turns off the Reynolds stress near the wall.

4.3 Cebeci's model for engineering flows.

As we have seen, Prandtl's mixing length idea is very useful in deriving theoretical profiles for geometrically simple flows. For geometrically more complex flow, the application of the model is complicated by the need to determine ℓ_{Mix} a-priori, because the mixing length has to be provided before solving the flow. An abundance of historical data can compensate for this disadvantage. A typical example is turbomachinery, where organizations can accumulate test data for gradually evolving designs over many decades. Even in these cases, however, the computed results are very sensitive to the selection of parameters like of the maximum mixing length, as shown in Figure 10 and even the best resourced organization may not have access to such detailed data.

5 Spalart-Allmaras Model

The Spalart-Allmaras model is the most popular representative of the family of one-equation models. The model was initially presented in 1992 in the paper:

P. Spalart and S. Allmaras, A one-equation turbulence model for aerodynamic flows, 30th Aerospace Sciences Meeting and Exhibit. January 1992, Reno (CO)

and represented an improvement on earlier one-equations models, such as the Baldwin-Barth model.

The main ingredient of the Spalart-Allmaras model is a transport equation for the eddy viscosity – or the modified eddy viscosity $\tilde{\nu}$. $\tilde{\nu}$ is generally known as the Spalart-Allmaras variable. The purpose of the transport equation is to account for the effect of the past history along the stramline on the structure of turbulence. This effect cannot be represented by algebraic models but is needed in boundary layers with pressure gradients, such as those on transonic aerofoils. The model does not attempt independent estimates for the TKE and the mixing length.

An interesting feature of the model, which can be seen in its derivation from the original publication, is that it is built in layers.

The first few terms are calibrated to represent the decay of homogeneous isotropic turbulence. Further terms are then added to calibrate the model with respect to establish results on free shear layers and ultimately boundary layers.

The governing equation of the model is reported below, together with the grouping of terms calibrated for different flows and a physical interpretation of each term:

$$\underbrace{\underbrace{\underbrace{\underbrace{\frac{\partial \tilde{\nu}}{\partial t} + U_j \frac{\partial \tilde{\nu}}{\partial x_j}}_{\text{Convection}} = \underbrace{c_{b1}\tilde{S}\tilde{\nu}}_{\text{Production}}}_{\text{Decay of homogeneous isotropic turbulence}} + \underbrace{\frac{1}{\sigma}\frac{\partial}{\partial x_j}\left((\nu+\tilde{\nu})\frac{\partial \tilde{\nu}}{\partial x_j}\right) + \frac{c_{b2}}{\sigma}\frac{\partial \tilde{\nu}}{\partial x_j}\frac{\partial \tilde{\nu}}{\partial x_j}}_{\text{Turbulent diffusion}}}_{\text{Free shear flows}} - \underbrace{c_{w1}f_w\left(\frac{\tilde{\nu}}{d}\right)}_{\text{Destruction near walls}}}_{\text{Boundary layers}}$$

The model is supplemented by the following auxiliary relations and constants

$$\nu_T = \tilde{\nu} f_{v1}, \qquad f_{v1} = \frac{\chi^3}{\chi^3 + c_{v1}^3}, \qquad \chi = \frac{\tilde{\nu}}{\nu},$$

$$c_{b1} = 0.1355, \quad c_{b2} = 0.622, \quad c_{v1} = 7.1, \qquad \sigma = 2/3$$

$$c_{w1} = \frac{c_{b1}}{\kappa^2} + \frac{(1+c_{b2})}{\sigma}, \quad c_{w2} = 0.3, \quad c_{w3} = 2, \quad \kappa = 0.41$$

$$f_{v2} = 1 - \frac{\chi}{1+\chi f_{v1}}, f_w = g\left[\frac{1+c_{w3}^6}{g^6 + c_{w3}^6}\right]^{\frac{1}{6}}, \qquad g = r + c_{w2}(r^6 - r)$$

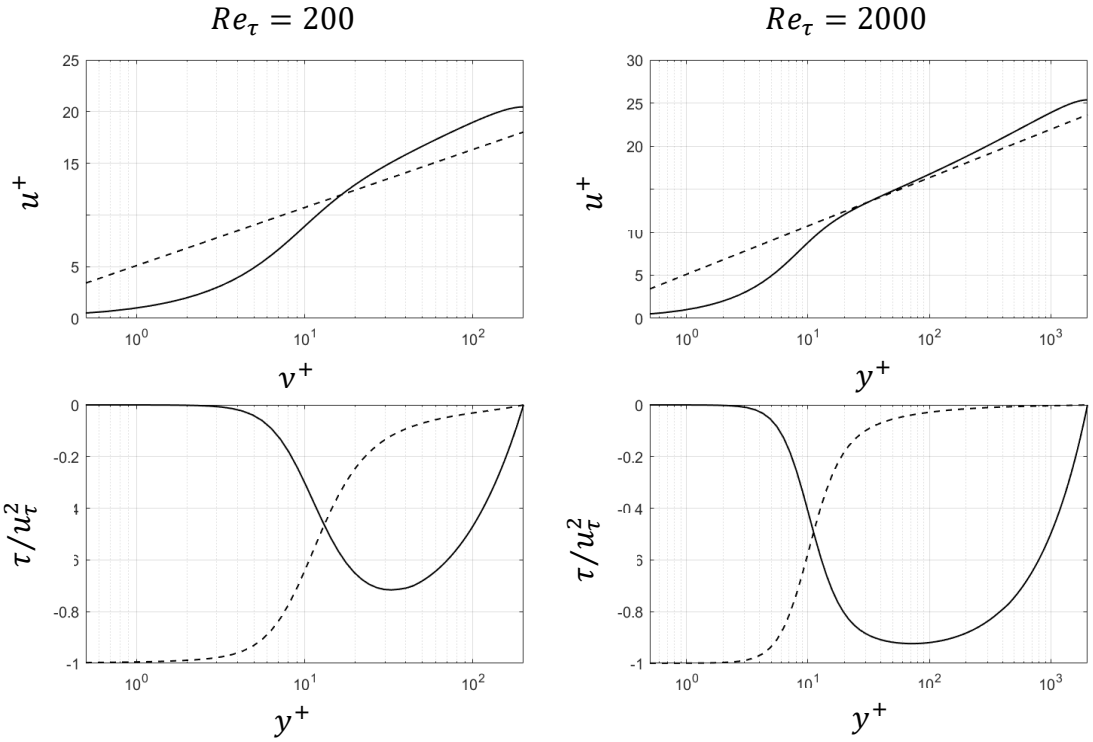

Figure 11: mean velocity profile and stress distributions from the Spalart-Allmaras model for turbulent channel flow at Re_τ 200 and 2000.

$$r = \frac{\tilde{\nu}}{\tilde{S}\kappa^2 d^2}, \qquad \tilde{S} = S + \frac{\tilde{\nu}}{\kappa^2 d^2} f_{v2}, \qquad S = \sqrt{2\Omega_{ij}\Omega_{ij}},$$

$\Omega = \frac{1}{2}\left(\frac{\partial U_i}{\partial x_j} - \frac{\partial U_j}{\partial x_i}\right)$ is the rotation tensor. d is distance from the closest wall. It is useful to point out at this stage that at high Reynolds numbers $\nu_T \to \tilde{\nu}$

5.1 Turbulent channel flow with Spalart's model

The properties of turbulent channel flows at $Re_\tau = 200$ and $Re_\tau = 2000$ are shown in Figure 11. The results show again that at low Reynolds number it is difficult to match the logarithmic law of the wall with an empirical model while the situation generally improves at higher Reynolds number.

We now inspect the variation of each term in the model equation for the channel flow. For this purpose we recast the model equation as follows:

$$0 = \underbrace{c_{b1}\tilde{S}\tilde{\nu}}_{P} + \underbrace{\frac{c_{b2}}{\sigma}\frac{\partial\tilde{\nu}}{\partial x_j}\frac{\partial\tilde{\nu}}{\partial x_j}}_{G} - \underbrace{c_{w1}f_w\left(\frac{\tilde{\nu}}{d}\right)^2}_{W} + \underbrace{\frac{1}{\sigma}\frac{\partial}{\partial x_j}\left(\tilde{\nu}\frac{\partial\tilde{\nu}}{\partial x_j}\right)}_{T} + \underbrace{\frac{\nu}{\sigma}\frac{\partial^2\tilde{\nu}}{\partial x_j\partial x_j}}_{D}$$

We can recognise P as similar to the production in the TKE budget, G and T as similar to the turbulent diffusion, W as similar to the dissipation rate ϵ and D as a viscous diffusion term. Figure 12 shows the variation of the Spalart variable $\tilde{\nu}$ and its

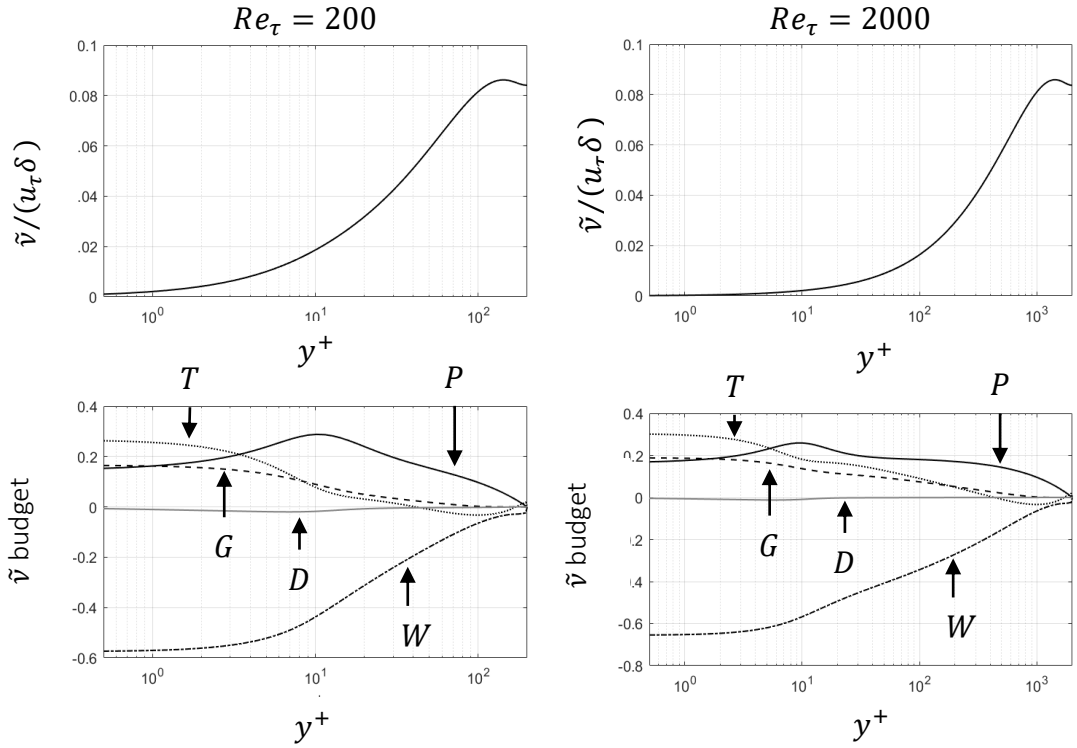

Figure 12: the Spalart variable and its budget in turbulent channel flow at $Re_\tau = 200$ and $Re_\tau = 2000$.

budget in turbulent channel flow at $Re_\tau = 200$ and $Re_\tau = 2000$. $\tilde{\nu}$ behaves not dissimilarly from the eddy viscosity inferred from a model such as the Cebeci model. It is interesting to see how the $\tilde{\nu}$ budget achieves this variation: the Spalart-Allmaras model never approximates equilibrium conditions, i.e. the turbulent production term P is never balanced just by the wall destruction term W. On the contrary, the combined effect of production and diffusion – turbulent and viscous – is needed to compensate for the near-wall destruction term. Also notice how the shape of the budget is invariant below $y^+ \approx 10$ which is the location of the peak production.